ANOTHER LOOK AT PATTERNS IN THE SURFACE ELECTRIC FIELD IN RELATION TO CLOUD-TO-GROUND

P1.2 LIGHTNING IN AIR-MASS THUNDERSTORMS OVER KENNEDY SPACE CENTER:

FALSE-ALARM RATES

Patrick T. Hyland*, Dustin E. Williams, William H. Beasley
University of Oklahoma, Norman, Oklahoma

1. INTRODUCTION

The success of operations at Kennedy Space Center (KSC) and Cape Canaveral Air Force Station (CCAFS) is highly sensitive to weather, most especially thunderstorms. Of particular concern are air-mass, or pulse, thunderstorms that develop over the complex, which can show very little sign of development in meteorological data prior to a first intra-cloud (IC) or cloud-to-ground (CG) lightning flash. The lightning produced by these storms not only threatens very complex and expensive machinery, but more importantly, it threatens the lives of those working in these conditions.

The KSC/CCAFS compound covers an area of approximately 650 square miles. 31 electric-field mills are deployed throughout this area (Figure 1). The Atlantic Ocean to the east and the Banana and Indian Rivers to the west border the area.

Current lightning hazard-warning guidelines are based on the consolidated wisdom of the lightning research community, derived from decades of experience. However, to the best of the authors' knowledge, no current lightning hazard-warning criteria incorporate objective application and interpretation of the temporal and spatial evolution of contours of electric field at the surface before, during, and after active lightning periods in thunderstorms.

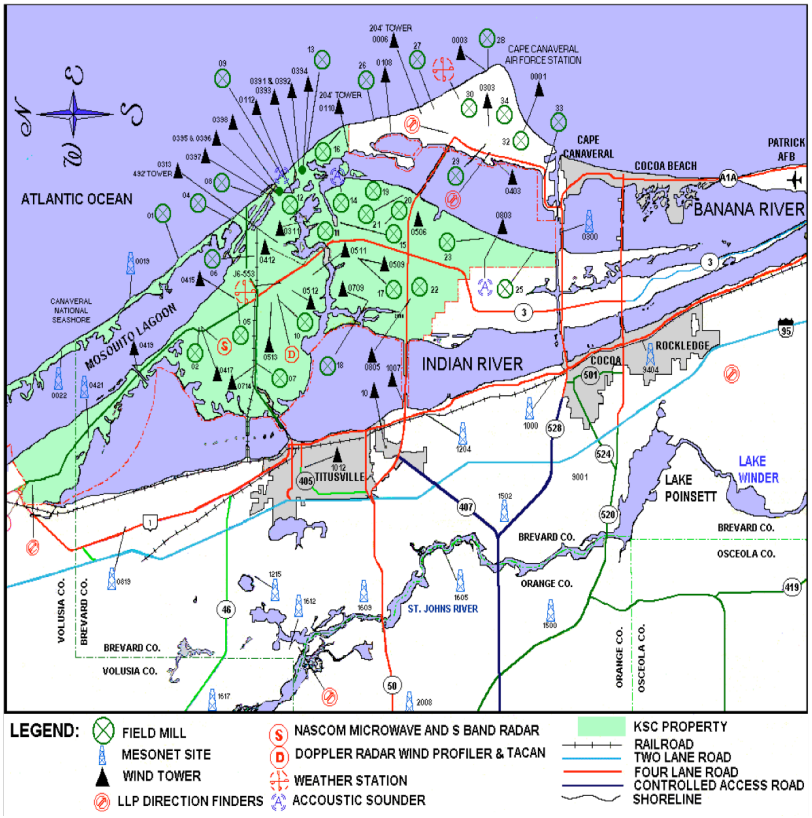

Figure 1. Kennedy Space Center and Cape Canaveral Air Force Station

One motivation for this study is recent research by Lengyel (2004), which showed that in more than half of 106 lightning casualty cases studied, the victims were struck by one of the first few CG flashes in a storm, or by one of the last few CG flashes in a storm. In both cases, knowledge of the electric field at the ground beneath storms is of critical importance to those charged with the responsibility of making hazard-warning decisions. In some cases (e.g. NASA/KSC) there is a need to know about the occurrence of first and last IC flashes as well.

Previously, the authors reported on the results of the analysis of contour animations of the electric field leading up to first CG flashes. It was noted that on the basis of this relatively limited data set, no consistent spatial and temporal patterns were found that would suggest where and when a CG flash would likely strike, respectively. However, the authors were able to show that the electric field at the ground

* *Corresponding author address*: Patrick T. Hyland, Univ. of Oklahoma, School of Meteorology, Norman, OK 73072-7307; e-mail: pat.hyland@ou.edu.

exceeded +/- 1 kV/m within 10 minutes and 10 km of the first CG flashes in 70 to 80 percent of the cases studied. This finding is consistent with the current lightning Launch Commit Criteria for Kennedy Space Center.

More recently, the authors have been working on the issue of the false-alarm rate (FAR). The FAR is of considerable importance in the development of any lightning-hazard warning criteria for the same reasons that the false-alarm rate is important for any weather-hazard warnings, such as those for tornadoes. The authors present herein some preliminary results of an attempt to define a usable FAR for CG lightning-strike warnings based on surface electric-field measurements.

2. PROCEDURE

The basic procedures used to identify suitable thunderstorm case studies follow the same procedures as before (Williams, Beasley, and Hyland 2008). First, it was decided to limit the study to the period between May 1 and September 30, which encompasses the majority of the warm season in central Florida, and represents the most active time of the year in Florida for "pulse" thunderstorms.

"Pulse" here means thunderstorms that develop fairly rapidly (on the order of tens of minutes) and most always occur near the peak in heating of the surface. These thunderstorms often develop while showing very little evidence of their onset in surface observations; i.e., they do not form on or follow a baroclinic boundary that can be easily detected through conventional observational data. However, these storms often form on low-altitude weak boundaries, such as sea-breeze fronts, river-breeze fronts, convective outflow, etc., and especially on intersections of two or more of these boundaries.

Second, it was decided to use data from years 2004 through 2006, a period for which the most reliable electric-field data were available.

Third, it was decided to limit the scope to the period of time between 1200 and 1800 EDT because pulse thunderstorms most often occur in the early to late afternoon during and just following the maximum positive net insolation and heating of the surface.

2.1 Thunderstorm Selection

In order to identify thunderstorms that fit the pulse criteria, KSC/CCAFS rainfall and CG lightning data were used first to identify days when there was either lightning observed somewhere within the Cloud-to-Ground Lightning Surveillance System (CGLSS) network, or rainfall over KSC, or in many cases both. The CGLSS data, which are accurate to within 250 m, were analyzed and the timing of all CG flashes between 1200 and 1800 EDT was noted. In a similar manner, the KSC/CCAFS rainfall data set was analyzed for the timing of rainfall over KSC/CCAFS. The rainfall data are reported every hour by the majority of the 31 field mills and give a total amount of rainfall that fell at that mill during the entire hour. If at any time between the hours of 1200 and 1800 EDT rainfall in any amount was recorded at any of the field-mill locations, that time was noted.

On the basis of rainfall and CG data, the authors chose days for which to create animations of radar data in order to examine the nature of the storms. Each day that rainfall and/or CG data were recorded, an animation of archived NEXRAD base reflectivity at tilt one (0.5°) from the Melbourne, Florida (KMLB) radar was created. The reflectivity images are in five-minute intervals. Enough base reflectivity data were used so that the entire time period of rainfall and/or CG data was covered, with a few minutes on either side. For example, if rainfall data were recorded from 1200 to 1400 and CG data were recorded from 1300 to 1600, then base reflectivity data from roughly 1155 to 1605 were animated.

Viewing the base reflectivity animations gave instant feedback on the manner in which a given thunderstorm formed. On many days, there were multiple thunderstorms that moved over KSC, so in order to be able to deduce the maximum amount of information from the surface electric field, one that evolves from a fair-weather electric field to that seen as the first CG flash occurs, only the first thunderstorm was examined. The time of this storm, based on when it developed and dissipated or advected away, was recorded. These times were recorded very liberally; that is, care was taken not to miss a first or last flash, so a generous period of time (on the order of 30 minutes) was allowed before and after the time of the thunderstorm.

Based on whether or not it fit the pulse criteria, each thunderstorm was determined to be either a suitable storm to examine or one that did not require further examination.

2.2 CG and Electric Field Data

For each case study thunderstorm, the timing and location of the first CG flash that occurred during the predetermined time of the storm, and within the area defined by KSC, was noted. This area is defined by a rectangle that is shaped by the lowest and highest latitude (east to west boundaries) and lowest and highest longitude (north to south boundaries) of the 31 field mills. Electric-field data were downloaded so that exactly 30 minutes before the first flash and 30 minutes after the last flash would be covered. The electric field data are measured at a 50-Hertz sample rate.

Given that in a 30-minute period there are 90000 electric field observations at each field mill, the data needed to be averaged to a much larger time step in order to be able to take a practical look at the field. It was decided that a 20-second time step would be appropriate because it would still show quite a bit of detail temporarily but only 90 plots per 30 minute time period would need to be created.

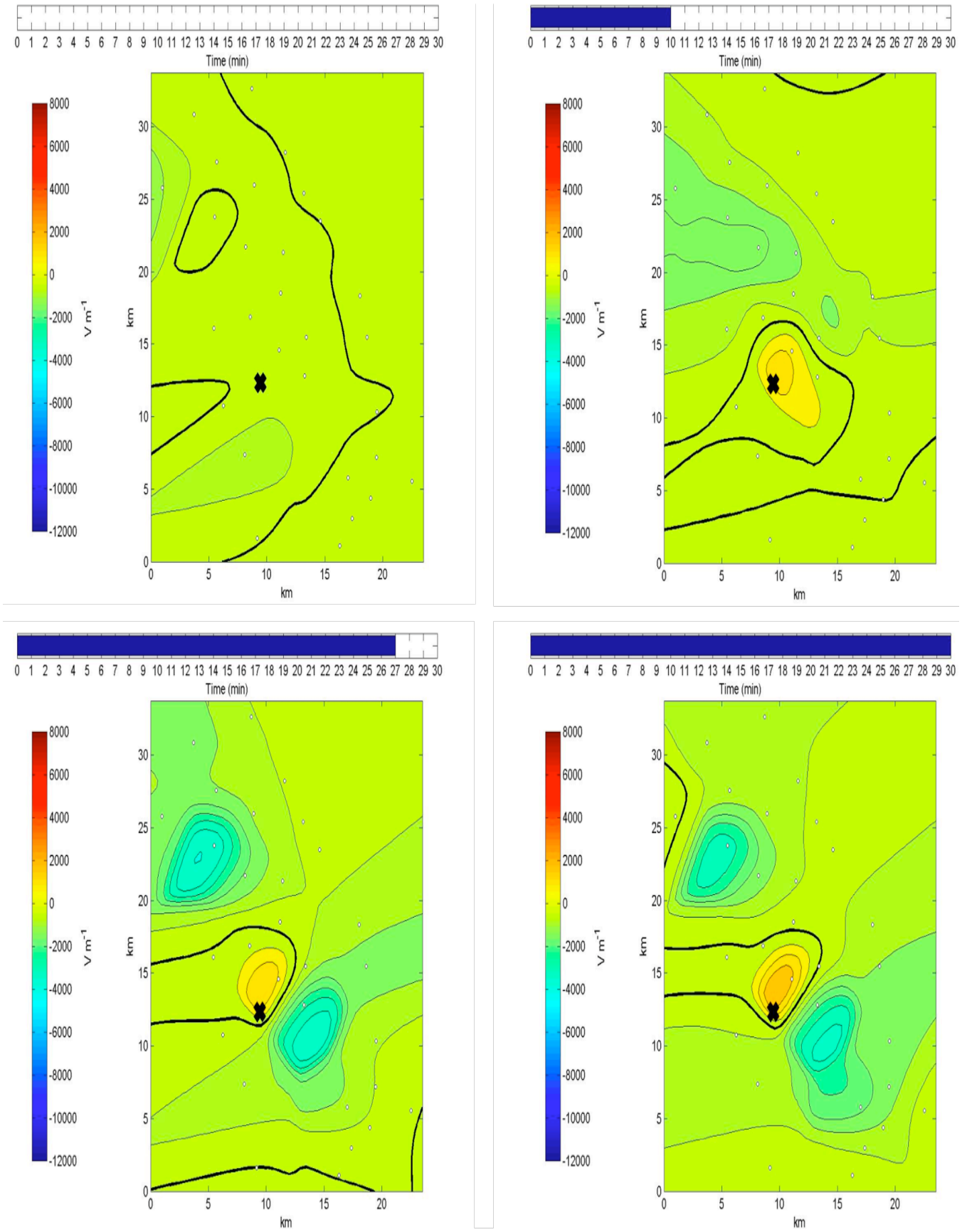

Figure 2. Example electric field contour images from 0, 10, 27, and 30 minutes. 30 minutes is the time at which the flash occurred. The circles represent the locations of the operational field mills and the X is the location of the CG flash. The bold contour is the 0 V/m isoline (Williams, Beasley, and Hyland, 2008).

The Air Force 45th Weather Squadron (45 WS) uses one-minute averages operationally at KSC/CCAFS, but that is done mostly for evaluating the lightning Launch Commit Criteria, as opposed to forecasting natural lightning.

If a given field mill was not operational at the start of the 30-minute period, or became inoperable at any point during the 30-minute time period, its data were not averaged and not used in the analysis. If all the field mills were not operational for any period of time during the 30-minute time period, then that CG flash was ignored and not analyzed.

A two-pass Barnes objective analysis was performed on the electric-field data. A first pass is computed, a bilinear interpolation is performed to estimate the first pass error, and then the second pass with an updated convergence parameter is computed, taking the estimated error into account. Using MATLAB, a filled-contour plot was produced for each of the 90 objectively analyzed electric-field data times. Also plotted were the locations of the operational field mills and the CG flash around which the 30 minutes worth of electric-field data is being plotted. These images were animated.

Figure 2 shows a sequence of contour images leading up to a first CG flash.

2.3 False-Alarm Rate (FAR)

In order to calculate the false-alarm rate, it was necessary to characterize events, hits, and misses. An event was defined in the following manner.

If the electric field at four adjacent grid points of the interpolated values within the KSC/CCAFS area exceeded the threshold of +/- 1, 2, or 5 kV/m for two consecutive time frames (the equivalent of a 40-second interval), then a MATLAB script determines where that instance occurred within the 30-minute time period. These four points are grid points calculated from the objective analysis described earlier. From this analysis, it is possible to determine whether or not to consider this instance as an event. If the start of the time interval trails the time of the first CG strike, then the instance is ignored. Otherwise, if the instance occurred within the time intervals of interest (0-3, 3-6, 6-9, 9-12, 12-15 minutes), then an event is recorded for each of the distances (1, 2, 5, and 10 km) for that particular time interval and electric-field threshold.

Hits and misses were defined in the following manner.

After an event is recorded, the MATLAB script accesses the CGLSS database and retrieves all the flashes that occurred during the time interval of interest. The locations of the flashes from the CGLSS database are provided in terms of latitude and longitude. These latitude and longitude readings are scaled to the x-y Cartesian grid used for this analysis. Following this conversion, the MATLAB script tests whether the flashes occurred within the four distances (1, 2, 5, and10 km) from the four adjacent points that exceeded the electric-field threshold. If a flash occurred within a designated distance, a hit is added to that particular distance, time interval, and electric-field threshold. Otherwise, a miss is recorded.

3. RESULTS

The number of events, hits, misses, and calculated false-alarm rate (FAR) with 3x3 grid spacing for readings that met or exceeded +/- 1 kV/m for various spatial and temporal intervals are presented in Table 1. Similar tables for other electric-field thresholds and different grid spacing are available.

Generally, the false-alarm rate averages 70 to 80 percent. While this number is slightly high, the false-alarm rate calculated here is similar to the false-alarm rate for the issuance of tornado warnings by the National Weather Service (McCarthy and Schaefer, 2002).

In an attempt to reduce the false-alarm rate, it was decided that extending the number of frames per second, which would increase the time step from 20 seconds to 40, 60, and 80 seconds, might lead to improvement in the false-alarm rate. Several tables showing the number of events, hits, misses, and false-alarm rate for different time steps, similar to those mentioned above, are also available. Overall, the false-alarm rate decreased when the time step was increased, albeit the increase was minor.

Table 1. Number of events, hits, misses, and calculated false-alarm rate (FAR) for readings that met or exceeded +/- 1 kV/m for various spatial and temporal intervals for 3x3 grid spacing.

+/- 1 kV/m (FAR_EPG_3x3)					
Events					
	0-3 min	*3-6 min*	*6-9 min*	*9-12 min*	*12-15 min*
1 km	1154226	941852	747354	578572	434402
2 km	1154226	941852	747354	578572	434402
5 km	1154226	941852	747354	578572	434402
10 km	1154226	941852	747354	578572	434402

+/- 1 kV/m (FAR_EPG_3x3)					
Hits					
	0-3 min	*3-6 min*	*6-9 min*	*9-12 min*	*12-15 min*
1 km	8032	6782	6722	5409	4234
2 km	19063	16497	15657	12513	10223
5 km	64536	57295	51042	41091	34757
10 km	167010	147036	124927	102057	82564

+/- 1 kV/m (FAR_EPG_3x3)					
Misses					
	0-3 min	*3-6 min*	*6-9 min*	*9-12 min*	*12-15 min*
1 km	1146194	935070	740632	573163	430168
2 km	1135163	925355	731697	566059	424179
5 km	1089690	884557	696312	537481	399645
10 km	987216	794816	622427	476515	351838

+/- 1 kV/m (FAR_EPG_3x3)					
False Alarm Rate (%)					
	0-3 min	*3-6 min*	*6-9 min*	*9-12 min*	*12-15 min*
1 km	99.30412	99.27993	99.10056	99.06511	99.02533
2 km	98.34842	98.24845	97.90501	97.83726	97.64665
5 km	94.40872	93.91677	93.1703	92.89786	91.99889
10 km	85.53056	84.38863	83.28409	82.36054	80.99364

4. CONCLUSION

The fact that the false-alarm rate (for the various temporal and spatial intervals as well as different electric-field thresholds and grid spacing) falls between 70 and 80 percent is at first disappointing, but in fact, this false-alarm rate is comparable to the false-alarm rate for tornado warnings by the National Weather Service. However, the intent of the authors was to evaluate the false-alarm rate in order to determine the feasibility and ease of use of electric-field mills in lightning hazard warning and detection. Due to the inherent unpredictability of lightning itself, it is difficult to justify a high false-alarm rate as a complete success. Electric-field mills only give one an indication of electric field at the surface. The net electric field at any point on the surface is the vector sum of the electric fields from all the charges in the storm overhead. Processes even within relatively less complicated air-mass thunderstorms are too complex and varying to enable one to determine features of the charge distribution above the surface from electrostatic field measurements alone. Future investigations using Lightning Mapping Array (LMA) and WSR-88D radar data may provide useful complementary information that could lead to a reduction in the false-alarm rate.

Reasons for the high false-alarm rate may lie in how an event was defined in the first place. Perhaps the number of events, as defined previously, is inherently high due to the distance of grid-point spacing considered. If one were to require the electric field to exceed a given threshold over a larger area, then it is likely that the number of events would be drastically reduced; therefore, a lower false-alarm rate would be expected.

In the future, it would be best to include an examination of the activity within thunderstorm clouds using radar and possibly Lightning Mapping Array data in addition to electric-field measurements at the surface in order to help find a predictive pattern in the surface contour animations of the electric field, and thus develop a comprehensive and reliable system in order to warn against lightning in a timely and accurate manner.

5. REFERENCES

Kennedy Space Center, 1995: Space shuttle weather launch commit criteria and KSC end of mission weather landing criteria. KSC press release 100-95, available online: http://www.pao.ksc.nasa.gov/kspao/release/1995/100-95.htm.

Lengyel, M., 2004: Lightning casualties and their proximity to surrounding cloud-to-ground lightning. M.S. Thesis, University of Oklahoma.

McCarthy, D. and J. Schaefer, 2002: Tornado trends over the past thirty years. Storm Prediction Center, available online: http://www.spc.noaa.gov/publications/mccarthy/tor30yrs.pdf.

Williams, D. E., W. H. Beasley, and P. T. Hyland, 2008: Analysis of surface electric-field contours before first and after last observed lightning flashes in air-mass thunderstorms over Kennedy Space Center. *Third Conf. On Meteorological Applications of Lightning Data*, New Orleans, LA, Amer. Meteor. Soc., 1-5.

6. ACKNOWLEDGEMENTS

The authors gratefully acknowledge the invaluable cooperation and advice of John T. Madura and Francis J. Merceret (NASA/KT-C-H, Kennedy Space Center) and William P. Roeder (U.S. Air Force 45th Weather Squadron, Patrick AFB). The authors also thank Aaron Bansemer (National Center for Atmospheric Research) for his significant contribution to the MATLAB code used for analysis.

This research was supported in part by a Research Initiation Grant from OK/NASA EPSCoR and in part by NASA EPSCoR grant #NNX07AV48A.